JOURNAL OF SOLID STATE CHEMISTRY 57, 43–58 (1985)

Interstitial Atoms in Metal–Metal Bonded Arrays: The Synthesis and Characterization of Heptascandium Decachlorodicarbide, $Sc_7Cl_{10}C_2$, and Comparison with the Interstitial-Free Sc_7Cl_{10}*

SHIOU-JYH HWU, JOHN D. CORBETT, AND KENNETH R. POEPPELMEIER

Ames Laboratory† and Department of Chemistry, Iowa State University, Ames, Iowa 50011

Received June 5, 1984; in revised form August 17, 1984

Reaction of Sc strips, $ScCl_3$, and graphite at 860–1000°C gives $Sc_7Cl_{10}C_2$ in quantitative yields, with transport occurring at the higher temperatures; adventitious carbon will also produce the phase. The compound has been shown to be isostructural with Er_7I_{10} by single-crystal X-ray diffraction (a = 18.620 (4) Å, b = 3.4975 (6) Å, c = 11.810 (2) Å, β = 99.81 (2)°; space group $C2/m$, $Z = 2$, $R = 0.029$, $R_w = 0.046$ for 676 reflections, Mo$K\alpha$, $2\theta < 50°$). The phase contains double chains of condensed scandium octahedra sharing edges with a carbon approximately centered in each ($\bar{d}$(Sc–C) = 2.31 Å) together with isolated scandium atoms in a parallel chain of chloride octahedra. The arrangement is very similar to that in the previously known Sc_7Cl_{10}, from which the heavy atom arrangement can be derived by displacement of all metal atoms by $b/2$ so as to convert chlorine functions on the metal chain from face-capping to edge-bridging. The driving force for this is thought to be the reduction of carbon–chlorine repulsive interactions. Core and valence XPS data for Sc_7Cl_{10}, $Sc_7Cl_{10}Cl_2$, Sc_2Cl_2C, $ScCl_3$, and Sc are presented to demonstrate the appearance of a carbide-like state for the interstitial, the presence of two different types of scandium in the first two compounds, the oxidation of the chain that accompanies the carbon insertion, and a substantial Sc–C covalency. The latter arises through mixing of the interstitial's 2s and 2p valence orbitals with metal–metal bonding cluster orbitals of the same symmetry.

Introduction

The many metal–metal bonded clusters, infinite chains, and double metal sheets that are known in reduced halides and chalcogenides have historically been believed to be free of anything within the metal-bounded interstices save for delocalized electrons. However, an increasing number of examples of nonmetals within M_6 cluster halides have been noted recently, first for a single hydrogen within Nb_6I_{11} (*1*) and $CsNb_6I_{11}$ (*2*) and then for second-period nonmetals in isolated clusters such as $Sc(Sc_6Cl_{12}N)$ (*3*) and in condensed clusters such as Gd_3Cl_3C (*4*) and Gd_4I_5C (*5*),[1] The

* Presented at the Symposium on Metal–Metal Bonding in Solid State Clusters and Extended Arrays, held during the American Chemical Society meeting, St. Louis, Missouri, April 9–10, 1984.

† Operated for the U.S. Department of Energy by Iowa State University under Contract W-7405-Eng-82. This research was supported by the Office of Basic Energy Sciences, Materials Sciences Division.

[1] There are in addition a number of lanthanide halides that contain dicarbon units in metal clusters or chains. According to simple electron counting, most of these phases are free of electrons for metal–metal bonding, and the clustering of the metals has been attributed principally to the strong metal–dicarbon bonding, for example, in $Gd_5Cl_9C_2$ (*6*) and $Gd_{12}I_{17}(C_2)_3$ (*7*).

0022-4596/85 $3.00

infinite double-metal-layered monohalides that represent the two-dimensional limit of cluster condensation have turned out to be particularly amenable substrates for this variety of reaction, forming Zr_2X_2H, MXH (*3, 8, 9*), M_2X_2C (*10, 11*), and $ZrXO_{0.3-0.4}$ (*12*) with X = Cl, Br and M = Sc, Y, or Zr. The nonmetal in this group is found in either the nominal tetrahedral (H, O) or octahedral (H,C) sites between the close-packed metal layers. The analogous lanthanide monohalides also form some derivatives of this sort (*13*).

The evident absence of interstitials in clusters composed of molybdenum and niobium family elements (except for hydrogen in the niobium iodides) probably results because of the small size of the metal and thence of the cavity available. On the other hand, the sizes of the *d* orbitals increase to the left in the periodic table and with a diminished number of cluster-based electrons for bonding, the clusters of earlier transition elements are larger and better able to accommodate small nonmetals without a great loss of metal–metal bonding through expansion. At the same time the nonmetals contribute bonding to a relatively electron-poor metal framework. Actually, this chemistry is not altogether unprecedented when considered in light of the properties of the metals themselves. Substantial amounts of these interstitials occur in α-phase (metal) solutions for some of the same group III and IV elements, for example, in $YH_{0.2}$, $ZrO_{0.4}$, and $ZrN_{0.3}$ (*14*), and many more binary but still metallic compounds are formed by these elements with a structural rearrangement of the parent metal. All of these reactions evidence strong metal–nonmetal interactions with substantial covalency, as has been demonstrated for the hydrides (*15*) and the carbides (*16*), for example.

Not surprisingly, some examples of interstitials within metal-bonded halide phases have been discovered serendipitously. The most likely circumstances are the accidental inclusion of a sufficient amount of an unexpected impurity, carbonaceous for example, together with the formation of a well-crystallized product that can be readily recognized and separated even in low yield. A residual electron density in the middle of a cluster following an otherwise satisfactory crystallographic solution is often the first hint that something may be amiss. Although X-ray diffraction is somewhat insensitive for the precise identification of the interstitial atom involved, synthesis of the same phase in high yield can invariably be accomplished by the purposeful addition of the correct nonmetal provided some mechanism for crystal growth is available. Some of the phases noted above have also been obtained through systematic explorations of the ternary systems. Fortunately, there are also a significant number of cluster and condensed cluster phases of the same metals that appear quite free of adventitious impurity atoms.

The present article describes the discovery and characterization of such a phase $Sc_7Cl_{10}C_2$ in which single carbon atoms are bound in the middle of all of the nominal Sc_6 octahedra that constitute the infinite double chains through sharing trans and some side edges of the simple clusters. The carbon-free analog Sc_7Cl_{10} is already known (*17*) with virtually identical metal chains but with a distinctly different arrangement of chlorine and of a separate scandium(III) chain. A better formulation that reflects the last feature is $^1_\infty[Sc^{III}Cl_2^+Sc_6Cl_8^-]$ when some approximations are made regarding the assignment of bridging chlorines between the units. Other known scandium chlorides are the related $^1_\infty[ScCl_2^+Sc_4Cl_6^-]$ with a single chain of edge-sharing scandium octahedra (*18*) and the double-metal-layered ScCl (*19*).

Some general properties of the condensed cluster systems containing the so-

called interstitial nonmetal atoms will also be considered for the chain and double-metal-sheet structures.

Experimental Procedures

The metal used was produced and distilled within the Ames Laboratory and had typical impurities (ppm atomic) of O—90, N—10, H—320, C—236, F—185, Fe—39, W—15, Y—2, Ce—3, Nd—7, other lanthanide, <2. This material was used either as rolled strips about 1 × 0.5 × 0.02 cm or as 100-mesh powder produced by decomposition of the ground hydride in high vacuum at 700–750°C (H : Sc = 0.09 : 1). Spectrographic grade powdered graphite (National brand, Union Carbide Corp.) was used as a source of carbon. The $ScCl_3$ preparation, typical reaction procedures in sealed Ta or Nb containers, the examination of products within the crystal-mounting glove box, the Guinier powder pattern techniques and least-squares lattice constant refinement therefrom, single-crystal X-ray diffraction techniques, and the photoelectron spectral measurements were carried out as previously described (*12, 15, 17–20*). The Guinier technique employing NBS silicon as an internal standard gave *a* and *c* lattice constants for NBS α-Al_2O_3 that agreed with the reference values within standard deviations of 0.8 and 2.5 parts in 10^4. The structure factor calculations and full matrix, least-squares refinements were carried out with the program ALLS (*21*) and the Fourier series calculations with FOUR (*22*).

Syntheses

The phase that was ultimately identified as $Sc_7Cl_{10}C_2$ was first seen as needles with a ruby-red reflectance that were obtained in low yield during an attempt to synthesize the composition "$RbSc_4Cl_6$" (*3*) through reaction of RbCl, Sc strips, and $ScCl_3$ at 1000/960°C for 5 weeks. The moisture-sensitive crystals were found in the hot end of the tube in a 10–15% yield. The principal new material otherwise was $Rb_3Sc_2Cl_9$ while ScOCl was not evident. Weissenberg photos together with the initial tuning procedures on the diffractometer showed these new crystals to be quite similar to Sc_7Cl_{10} (*17*) with the same space group (*C2/m*) but with somewhat different values for one axis length and the monoclinic angle. The Guinier powder pattern of the new phase was quite different.[2]

The crystal structure solution (below) showed this new phase had a Sc_7Cl_{10}-like double metal chain structures but with a distinctly different arrangement of both the chlorine atoms and the scandium(III) side chain and with a clear electron density residual in the center of each metal cluster within the chain. The last was initially taken to represent oxygen (and was refined as such) because of the rather pervasive character of ROCl oxychloride in this and other rare earth metal-rich systems where it is thought to come both from the reactants and from some outgassing of the silica jacket (*23*) unless this is flamed especially well before sealing. Microprobe analyses of three single crystals supported on a graphite disk gave good agreement for the chlorine-to-scandium ratio, 1.42 (3) : 1 vs 1.43 : 1 for Sc_7Cl_{10}, but the O : Cl values ranged between 0.06 and 0.48 : 1. More importantly, attempts at direct synthesis in which ScOCl was purposely included gave inconsistent results, the "$Sc_7Cl_{10}O_2$" being found in some instances but not in many others. ScOCl was clearly mobile at these tempera-

[2] The stronger 40% of the diffraction lines observed for $Sc_7Cl_{10}C_2$ by Guinier techniques are, in 2θ ($CuK\alpha_1$) with relative intensities in parenthesis: 13.28 (50), 29.75 (70), 30.59 (15), 34.07 (30), 34.42 (100), 35.94 (40), 36.98 (20), 39.14 (80), 51.27 (20), 52.25 (90), 53.30 (30), 53.82 (50). Some intensity variations from theory are to be expected because of preferred orientation of the needles on the mounting tape.

tures so a kinetic explanation for the lack of success did not seem appropriate. A second structural result was meanwhile obtained for a crystal from a 5–10% yield in a reaction that also produced interstitial-free Sc_5Cl_8.

A clue to the correct identity of the interstitial atoms came from another reaction in which crystals of the phase in question were found together with single crystals of what was subsequently structurally refined as and shown to be Sc_2Cl_2C by its direct synthesis in high yield from metal, trichloride, and graphite (*10*). Reactions aimed at the synthesis of $Sc_2Cl_2C_x$ from the same reactants (excess Sc strips) at 1010°C gave a mixture of Sc_2Cl_2C and $Sc_7Cl_{10}C_2$ for $x \leq \sim 0.8$, with a quantitative yield of large crystals of the latter at the correct chlorine-to-carbon stoichiometry ($x = 0.4$). A third set of diffraction data was collected and refined for a single crystal from the last reaction to confirm that the known phase was the same as studied twice before.

Reaction of the above starting materials (excess strips) for a week at 860°C is sufficient to give microcrystalline products of $Sc_7Cl_{10}C_2$, with transport yielding nice single crystals over a longer period near 1000°C. A stoichiometric amount of powdered metal gives Sc_2Cl_2C and unreacted $ScCl_3$ after 6 weeks at 860°C, presumably representing a nonequilibrium situation. It appears that Sc_5Cl_8, $Sc_7Cl_{10}C_2$, and Sc_2Cl_2C are adjacent line phases, with the yields at 1000°C depending principally on the relative amount of carbon present; characteristically, scandium strips in excess are needed for good yields. The preparation of Sc_7Cl_{10} instead of Sc_5Cl_8 is generally carried out at lower temperatures, 860–900°C, and with powdered metal (*17*). A powdered scandium reactant also appears necessary to obtain ScCl.

TABLE I

CRYSTAL AND REFINEMENT DATA FOR THREE CRYSTALS OF $Sc_7Cl_{10}C_2$, SPACE GROUP $C2/m$ (~20°C)

	1[a]	2		3[b]	
Crystal size, mm	0.5 × 0.05 × 0.02	0.4 × 0.04 × 0.02		0.5 × 0.06 × 0.03	
Lattice parameters, Å					
a	18.634 (2)	18.620 (4)[c]		18.613 (5)	
b	3.5131 (4)	3.4975 (6)		3.4960 (7)	
c	11.834 (1)	11.810 (2)		11.806 (2)	
β (deg)	99.77 (1)	99.81 (2)		99.78 (2)	
Cell vol. (Å^3)	763.4 (1)	757.9 (2)		757.1 (3)	
Octants measured	4	4		4	
2θ limit, deg. (Mo$K\alpha$)	50	50		55	
Indep. refl. ($>3\sigma(I)$)	630	676		426	
R(ave)	0.042	0.024		0.024	
Carbon occupancy	2.46 (5)	2.17 (5)	2.0[d]	2.57 (8)	2.20 (4)
B(Å^2)	1.0 (1)	1.2 (2)	0.8 (1)	3.8 (5)	0.77[d]
R	0.035	0.029	0.029	0.038	0.040
R_w	0.046	0.046	0.047	0.041	0.044
$\bar{d}$, Sc–C, Å	2.33	2.31		2.31	

[a] Crystals in the order cited under Syntheses section.

[b] Data taken on Syntex $P2_1$ diffractometer with a θ–2θ scan; the other two studies utilized an Ames Laboratory instrument in an Ω-scan mode.

[c] Guinier data, Cu$K\alpha$.

[d] Parameter fixed; the B is an average of the isotropic values for Sc and Cl.

TABLE II

ATOM PARAMETERS FOR $Sc_7Cl_{10}C_2$, CRYSTAL 2[a]

	x	y	z	B_{11}[b]	B_{22}	B_{33}	B_{13}
Sc1	0.0	0.0	0.0	0.76 (6)	1.49 (8)	0.86 (7)	0.19 (5)
Sc2	0.3464 (1)	0.0	0.2676 (1)	0.85 (5)	0.63 (5)	0.88 (5)	0.25 (4)
Sc3	0.2004 (1)	0.5	0.2768 (1)	0.75 (5)	0.58 (5)	0.79 (5)	0.17 (3)
Sc4	0.3190 (1)	0.5	0.4928 (1)	0.70 (5)	0.41 (5)	0.79 (5)	0.19 (4)
Cl1	0.4284 (1)	0.5	0.3742 (1)	0.88 (6)	0.90 (6)	1.23 (6)	0.18 (5)
Cl2	0.0956 (1)	0.5	0.3843 (1)	0.79 (6)	0.96 (7)	1.03 (6)	0.18 (4)
Cl3	0.1239 (1)	0.0	0.1336 (1)	1.37 (6)	0.91 (7)	1.32 (6)	−0.24 (5)
Cl4	0.2871 (1)	0.5	0.1255 (1)	1.17 (6)	0.78 (6)	0.92 (6)	0.20 (4)
Cl5	0.4519 (1)	0.0	0.1243 (1)	1.63 (7)	0.91 (7)	1.55 (6)	0.72 (5)
C[c]	0.2613 (3)	0.0	0.3745 (5)	1.2 (2)			

[a] Space group $C2/m$ (No. 12).

[b] $T = \exp[(-1/4)(B_{11}h^2a^{*2} + B_{22}k^2b^{*2} + B_{33}l^2c^{*2} + 2B_{12}hka^*b^* + 2B_{13}hla^*c^* + 2B_{23}klb^*c^*)]$, $B_{12} = B_{23} = 0$.

[c] Occupancy of 2.17 (5).

Structure Solutions

Although the cell parameters of the new phase were clearly different from those of Sc_7Cl_{10}, a sharpened Patterson map showed that many of the same structural features remained according to the u,0,w and u, 1/2,w sections. The atomic coordinates for the related (see below) structure of Er_7I_{10} (*24*) provided the correct model, and this refined uneventfully to a very satisfactory result. Crystal parameters and some refinement results for this and two crystals subsequently studied (and referred to in the previous section) are given in Table I. Absorption corrections were applied to all using a ϕ-scan method and the program ABSN (*25*), with scans being made at two different values of θ for the first two crystals ($\mu = 47$ cm^{-1}, $0.83 < T < 0.99$ for crystal 2). Secondary extinction corrections were found to be unnecessary. The final difference maps were flat to well less than 1 e/Å^3 at all positions.

Refinement of diffraction data from a third crystal was completed in order to establish that the product made in high yield by the purposeful introduction of carbon was identical to those twice studied that contained uncertain interstitials (though clearly the occupancies in these two cases refined to close to the correct values for carbon). The last study accomplished this purpose well although the standard deviations of the positional and thermal parameters were two to four times greater than obtained with either of the other crystals. The poorer result likely arose from somewhat lower crystal perfection relative to crystal 2 and, more importantly, because fewer reflections were observed with a θ–2θ scan mode and no monochromator (Table I). Weissenberg photos indicated the crystal quality was 2 > 3 > 1 although the differences were not large and all would be characterized as satisfactory as to peak size and freedom from more than slight streaking. The question of different cell sizes will be considered later.

The refined structural parameters for the second crystal of $Sc_7Cl_{10}C_2$, which appears to be the best result of the three studied by all criteria, are listed in Table II. The observed and calculated structure factor data appears in Table III.

The composition of $Sc_7Cl_{10}C_2$, especially

TABLE III

Observed and Calculated Structure Factors (×10) for $Sc_7Cl_{10}C_2$, Crystal 2

K = -4																																			
H	L	FO	FC	-8	5	134	164	-9	9	1725	1734	-10	5	183	190	6	6	127	100	5	4	250	257	4	4	1209	1193
-6	1	122	149	-8	6	290	275	-9	10	935	939	-10	6	385	372	6	8	353	328	5	5	377	366	6	5	1880	1868
-4	2	207	225	-8	8	857	881	-9	11	471	457	-10	7	100	127	6	9	393	382	5	6	615	600	6	8	294	285
-2	2	210	214	-8	9	474	460	-7	0	90	86	-10	8	231	240	6	10	940	937	5	7	952	929	6	9	504	489
-2	3	324	327	-8	10	343	342	-7	1	538	547	-10	9	126	112	6	11	616	618	5	8	867	897	6	10	810	803
0	1	164	153	-6	1	176	175	-7	2	129	125	-10	11	190	118	8	0	893	904	5	10	265	239	8	1	1363	1406
2	-1	94	113	-6	2	758	753	-7	3	420	414	-10	13	254	257	8	1	1868	1932	5	11	345	332	8	2	350	360
6	0	362	145	-6	3	1838	1766	-7	4	199	201	-8	1	100	99	8	2	431	454	5	12	325	329	8	3	217	225
				-6	4	2220	2203	-7	6	647	647	-8	2	581	599	8	3	270	283	7	1	347	362	8	5	1096	1098
K = -3				-6	5	419	408	-7	10	428	412	-8	3	1116	1092	8	5	1323	1409	7	2	396	394	8	6	215	185
H	L	FO	FC	-6	6	419	434	-7	12	118	157	-8	4	524	521	8	6	218	222	7	4	210	196	8	8	133	159
-15	1	253	207	-6	7	805	785	-7	13	254	251	-8	5	219	232	8	7	113	90	7	5	268	271	8	9	618	626
-15	2	100	163	-6	8	387	375	-5	1	971	981	-8	6	398	388	8	8	203	209	7	6	91	129	8	10	732	748
-15	3	513	490	-6	9	724	733	-5	2	1889	1837	-8	7	1039	993	8	9	771	739	7	7	851	848	10	0	438	445
-13	0	125	45	-6	10	382	377	-5	4	165	155	-8	8	1019	1060	8	10	872	846	7	8	122	152	10	1	423	419
-13	1	230	240	-6	11	419	443	-5	5	135	157	-8	9	578	560	8	12	309	320	7	9	246	236	10	2	474	493
-13	5	432	419	-6	12	1231	1292	-5	6	679	693	-8	10	424	419	10	0	596	592	7	10	207	192	10	3	92	131
-11	1	624	608	-4	1	295	302	-5	10	998	998	-8	13	412	415	10	1	519	523	9	0	493	487	10	4	192	194
-11	2	366	358	-4	2	437	432	-5	11	348	346	-6	1	278	264	10	2	627	645	9	3	308	336	10	5	186	180
-11	3	308	305	-4	3	241	245	-5	13	351	363	-6	2	1123	1114	10	3	175	187	9	4	442	449	10	6	262	264
-11	4	264	300	-4	5	253	235	-3	1	464	474	-6	3	2637	2571	10	4	248	261	9	5	258	241	10	8	144	192
-11	5	712	741	-4	6	268	261	-3	2	804	750	-6	4	3157	3118	10	5	231	232	9	6	376	359	10	9	470	471
-11	6	915	928	-4	7	257	259	-3	3	1698	1616	-6	5	991	972	10	6	347	337	9	7	1976	1921	12	0	135	119
-11	7	150	127	-4	8	329	329	-3	4	1471	1462	-6	6	559	544	10	7	105	104	9	8	185	198	12	1	1667	1674
-9	1	2063	2071	-4	9	684	661	-3	5	1044	1019	-6	7	1048	1013	10	8	232	230	9	10	248	250	12	2	773	771
-9	2	469	458	-4	10	253	251	-3	6	2773	2803	-6	8	520	497	10	9	527	534	9	11	650	633	12	3	606	622
-9	3	134	142	-4	12	240	242	-3	7	624	638	-6	9	882	864	10	10	730	725	11	0	442	432	12	4	301	324
-9	4	122	62	-2	1	262	256	-3	9	237	232	-6	10	676	672	12	0	106	121	11	1	613	601	12	5	846	864
-9	5	468	438	-2	2	458	446	-3	10	623	616	-6	11	525	502	12	1	2033	2073	11	2	571	586	12	6	128	154
-9	6	425	452	-2	3	632	604	-3	11	1249	1252	-6	12	1484	1493	12	2	941	975	11	3	858	883	12	8	411	414
-9	7	271	275	-2	4	849	816	-3	12	368	365	-6	13	309	296	12	3	771	779	11	4	1192	1222	14	0	323	320
-9	8	650	668	-2	5	754	744	-1	1	240	236	-4	1	483	479	12	4	394	394	11	5	310	301	14	1	878	883
-7	1	302	310	-2	6	350	327	-1	2	1604	1529	-4	2	687	665	12	5	1011	1031	11	6	165	177	14	2	420	413
-7	3	234	236	-2	8	216	230	-1	3	453	458	-4	3	389	384	12	6	201	192	11	7	598	589	14	3	116	87
-7	4	96	118	-2	9	242	242	-1	5	377	375	-4	4	151	135	12	8	482	468	11	8	711	707	14	4	129	151
-7	6	422	413	-2	10	139	160	-1	6	956	956	-4	5	326	350	12	9	764	758	13	1	204	216	14	5	541	515
-5	1	615	591	-2	11	125	84	-1	7	249	253	-4	6	382	380	12	10	672	690	13	3	961	948	14	6	717	704
-5	2	1069	1055	-2	12	270	270	-1	8	203	216	-4	7	340	339	12	-10	117	110	13	4	544	561	16	0	168	159
-5	3	147	91	10	-5	119	133	-1	9	272	256	-4	8	405	394	14	0	424	403	13	5	261	247	16	1	90	111
-5	6	410	418	14	-1	100	7	-1	10	423	439	-4	9	834	817	14	1	1048	1089	13	6	172	150	16	2	355	398
-3	1	284	283	16	-1	141	122	-1	11	706	686	-4	10	316	310	14	2	508	487	13	7	150	152	16	3	316	317
-3	2	365	329	18	-4	125	108	-1	12	290	316	-4	12	283	262	14	3	94	95	13	9	316	314	18	1	265	291
-3	3	930	913					-1	13	296	312	-4	13	461	444	14	4	192	202	15	0	714	704	18	2	660	669
-3	4	827	832	K = -1				7	-9	93	96	-2	1	493	443	14	5	605	612	15	1	431	426				
-3	5	623	605	H	L	FO	FC	19	-3	106	120	-2	2	733	732	14	6	812	802	15	2	809	781	K = 3			
-3	6	1864	1834	-21	4	967	983	21	-2	217	180	-2	3	918	920	14	7	509	489	15	3	1038	1042	H	L	FO	FC
-3	7	391	391	-21	5	274	263					-2	4	1157	1159	14	8	612	614	15	4	932	922	-7	-4	125	118
-3	9	170	175	-19	1	649	657	K = 0				-2	5	1044	1042	14	9	371	379	15	5	279	258	1	1	227	219
-1	1	139	169	-19	2	131	120	H	L	FO	FC	-2	6	443	461	14	-9	93	111	15	7	434	426	1	2	263	262
-1	2	858	822	-19	4	137	113	-22	2	527	533	-2	8	294	295	16	0	186	196	15	8	638	652	1	3	157	102
-1	3	307	293	-19	5	581	594	-22	3	206	194	-2	9	339	319	16	1	106	115	17	0	992	1002	1	5	182	145
-1	5	215	211	-19	6	121	64	-20	2	476	482	-2	10	194	207	16	2	421	428	17	2	307	296	1	6	543	553
-1	6	398	388	-19	8	140	161	-20	3	453	447	-2	11	90	108	16	4	88	68	17	3	178	151	1	7	247	271
-1	7	168	179	-17	1	743	730	-20	4	325	312	-2	12	305	308	16	5	362	352	17	4	861	854	1	8	118	125
-1	8	137	140	-17	2	236	211	-20	6	533	509	-2	13	499	513	16	6	1080	1044	17	5	127	141	1	9	235	226
-1	9	154	155	-17	3	591	581	-20	7	1064	1096	-2	14	83	61	16	7	187	205	19	0	719	719	3	1	373	379
3	-5	108	82	-17	4	515	526	-18	0	90	80	-2-11		113	94	18	1	338	346	19	1	367	372	3	2	1818	1822
3	-4	101	114	-17	5	483	475	-18	1	633	623	0	1	403	376	18	2	765	766	19	2	246	241	3	3	1437	1423
				-17	6	259	261	-18	2	1495	1467	0	2	319	321	18	4	213	207	19	3	280	270	3	4	523	512
K = -2				-17	7	293	284	-18	3	414	411	0	3	152	174	18	5	108	96	19	4	166	172	3	5	364	364
H	L	FO	FC	-17	8	482	455	-18	4	740	717	0	4	684	641	18	6	1017	1018	21	0	816	827	3	6	661	633
-18	1	536	528	-17	9	887	910	-18	8	353	361	0	5	1068	1062	18	-7	92	91					3	7	384	400
-18	2	1246	1254	-17	10	702	693	-18	9	706	729	0	6	87	74	20	0	408	413	K = 2				3	8	371	370
-18	3	355	361	-15	1	252	259	-18	10	890	913	0	7	900	902	20	1	488	520	H	L	FO	FC	3	9	525	537
-18	6	623	625	-15	2	201	192	-16	1	169	165	0	8	2541	2549	20	2	518	502	-4	-5	125	93	5	0	160	168
-16	2	655	665	-15	3	657	647	-16	2	799	803	0	9	923	894	20	3	607	617	-2	-10	103	103	5	1	366	367
-16	3	446	440	-15	4	742	755	-16	3	546	508	0	10	376	370					0	0	3493	3684	5	2	615	616
-16	4	321	329	-15	5	1653	1647	-16	4	399	395	0	11	178	163	K = 1				0	1	251	237	5	3	502	501
-16	5	125	148	-15	6	267	270	-16	5	159	186	0	12	703	702	H	L	FO	FC	0	2	228	211	5	4	106	137
-16	6	187	182	-15	7	408	390	-16	6	227	222	0	13	479	476	-15	-6	86	34	0	3	143	137	5	5	189	192
-16	7	107	116	-15	8	760	755	-16	7	144	120	2	0	716	670	1	1	429	435	0	4	349	331	5	6	383	394
-16	8	228	242	-15	9	144	139	-16	8	299	285	2	1	974	962	1	2	322	321	0	5	810	798	5	7	644	671
-14	2	493	470	-15	10	569	586	-16	9	123	119	2	2	713	735	1	3	202	209	0	7	681	687	5	8	603	640
-14	3	1305	1262	-15	11	351	372	-16	10	204	210	2	3	469	477	1	4	108	105	0	8	2055	2041	7	1	197	194
-14	4	422	413	-13	1	373	367	-14	2	549	556	2	4	776	792	1	5	291	289	0	9	748	740	7	2	215	226
-14	5	211	204	-13	3	215	182	-14	3	1622	1557	2	5	1591	1642	1	6	877	886	0	10	308	304	7	5	174	167
-14	6	146	174	-13	5	622	609	-14	4	492	476	2	7	222	207	1	7	357	359	0	11	110	125	7	7	593	594
-14	7	605	635	-13	6	114	101	-14	5	251	238	2	8	367	361	1	8	193	197	0	12	602	610	9	0	279	294
-14	8	253	264	-13	7	211	227	-14	6	231	225	2	9	928	929	1	9	356	333	2	0	424	423	9	3	436	406
-12	1	204	201	-13	8	143	164	-14	7	760	760	2	10	103	108	1	10	185	205	2	1	560	585	9	4	312	340
-12	2	117	114	-13	9	217	211	-14	8	282	296	2	12	214	225	1	11	376	374	2	2	461	456	9	5	169	182
-12	3	760	736	-13	10	123	158	-14	10	142	147	2	13	819	819	1	13	210	198	2	3	315	321	9	6	239	242
-12	4	860	851	-13	11	146	165	-14	11	896	941	4	0	466	487	3	0	96	95	2	4	592	591	11	0	256	265
-12	5	662	676	-11	1	872	887	-14	12	710	715	4	1	1027	1073	3	1	639	669	2	5	1200	1195	11	1	369	372
-12	6	160	155	-11	2	582	578	-12	1	279	287	4	2	391	399	3	2	3157	3260	2	7	190	177	11	2	379	400
-12	7	1595	1596	-11	3	302	302	-12	2	164	155	4	3	97	92	3	3	2499	2508	2	8	320	306	11	3	623	633
-12	8	550	543	-11	4	442	450	-12	3	917	921	4	4	637	636	3	4	873	886	2	9	734	733	11	4	840	860
-12	9	98	103	-11	5	1015	1041	-12	4	1081	1071	4	6	360	348	3	5	569	564	2	11	85	78	11	5	178	195
-12	10	94	99	-11	6	1352	1323	-12	5	872	853	4	9	494	491	3	6	964	968	4	0	325	330	13	3	667	675
-10	1	102	100	-11	7	208	214	-12	6	205	200	4	10	182	183	3	7	623	623	4	1	673	694	15	0	508	497
-10	2	129	163	-11	8	110	144	-12	7	1889	1891	4	12	429	419	3	8	465	477	4	2	231	248				
-10	3	260	263	-11	10	602	597	-12	8	673	664	4	13	363	359	3	9	741	714	4	4	430	450	K = 4			
-10	4	141	129	-9	1	3280	3294	-12	9	98	105	4-11		103	104	3	10	825	818	4	6	259	259	H	L	FO	FC
-10	6	266	289	-9	2	722	703	-12	11	836	827	6	0	299	319	3	11	1313	1310	4	9	400	402	0	0	1940	2013
-10	8	198	192	-9	3	186	195	-12	12	948	968	6	1	808	806	3	13	372	358	4	10	169	144	0	2	141	127
-10	10	135	139	-9	5	583	590	-10	1	181	154	6	2	1170	1211	5	0	304	311	6	0	291	288	2	0	259	261
-8	2	403	419	-9	6	629	629	-10	2	238	247	6	3	1466	1520	5	1	645	678	6	1	435	448	2	1	275	295
-8	3	763	784	-9	7	424	405	-10	3	366	357	6	4	1579	1630	5	2	1016	1093	6	2	791	838	2	2	215	224
-8	4	421	397	-9	8	969	955	-10	4	210	193	6	5	2391	2412	5	3	773	803	6	3	1063	1082	2	3	155	184
																								4	0	235	210
																								4	1	380	376

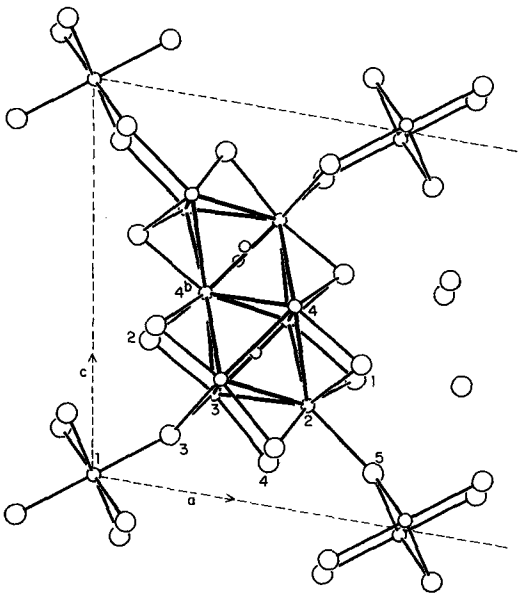

FIG. 1. A section of the $Sc_7Cl_{10}C_2$ structure viewed approximately along the metal chain [010] plus the atom numbering system. All atoms occur at $y = 0$ or 1/2, with pairs of circles corresponding to those with $y = \pm 1/2$. Heavy lines interconnect the metal atoms (small spheres). The remainder of the cell is generated by a C-centering condition ($x + 1/2$, $y + 1/2$, z); an inversion center occurs at the midpoint of the Sc4–Sc4^b connections.

the identity and amount of the carbon interstitial, was established principally by the synthesis of the phase in substantially quantitative yield (>95%, with no other phases detected in Guinier patterns) by the on-stoichiometry reaction

$$10\ ScCl_3 + 6\ C + 11\ Sc \text{ (excess, strips)} \rightarrow 3\ Sc_7Cl_{10}C_2.$$

The X-ray refinements agreed with this fairly well (Table I). In addition, the presence of a carbide-like C 1*s* emission from the compound was established by photoelectron spectroscopy (below). Powder pattern data show that the same phase had been seen earlier (*18*) and found to have Cl : Sc = 1.40 (7) on the basis of microprobe analyses.

Structure Description

Figure 1 shows the contents of approximately one-half of the C-centered unit cell as viewed along the short *b* axis but with the cell tilted slightly so the clusters and bridging functions may be discerned. All atoms occur at $y = \pm 1/2$ (double circles) or $y = 0$ (single). The scandium atom arrangement, basically the same as in Sc_7Cl_{10}, can be viewed as first generating elongated octahedra which share trans edges (Sc3–Sc4) so to form chains parallel to *b*. In addition, parallel pairs of these chains are fused through sharing of a pair of cis edges in each octahedron (Sc4–Sc4^b) to yield double chains. Carbon is near the center of each octahedron. Side and top views of the metal chain (plus carbon) are shown in Fig. 2 with all of the shared edges in heavy outline in the bottom drawing. One octahedron can be described as $(Sc2)(Sc3)_{2/2}(Sc4)_{2/3}(Sc4)_{1/3}$.

Two additional features define the structure, the halogen placement about both the metal chain and the isolated Sc1 atoms which are located at the corners and at the center of the (0,0,1) face. These arrangements are significantly different from those in Sc_7Cl_{10}. As can be seen in Fig. 1, chlorine bridges all exposed *edges* of the octahedra that comprise the chains to produce a $^1_\infty[Sc_6Cl_6]$ unit. Second, the isolated Sc1 atoms which are again taken to be scandium(III) are surrounded by chlorine octahedra. Since these have the same period as the metal chain, the chlorine octahedra also share trans edges (Cl5–Cl5) and generate commensurate $Sc1(Cl3)_2(Cl5)_{4/2}$ octahedral chains. These metal and Sc-based chains are not independent, however. All chlorine in the structure are three-coordinate to scandium, achieving this either through bridging pairs of edges of the fused metal octahedra along the chain (Cl1,2,4) or by being part of the $ScCl_2Cl_{4/2}$ chains *and* occupying the remaining, all-important exo positions on the metal chain. Thus the Cl3 api-

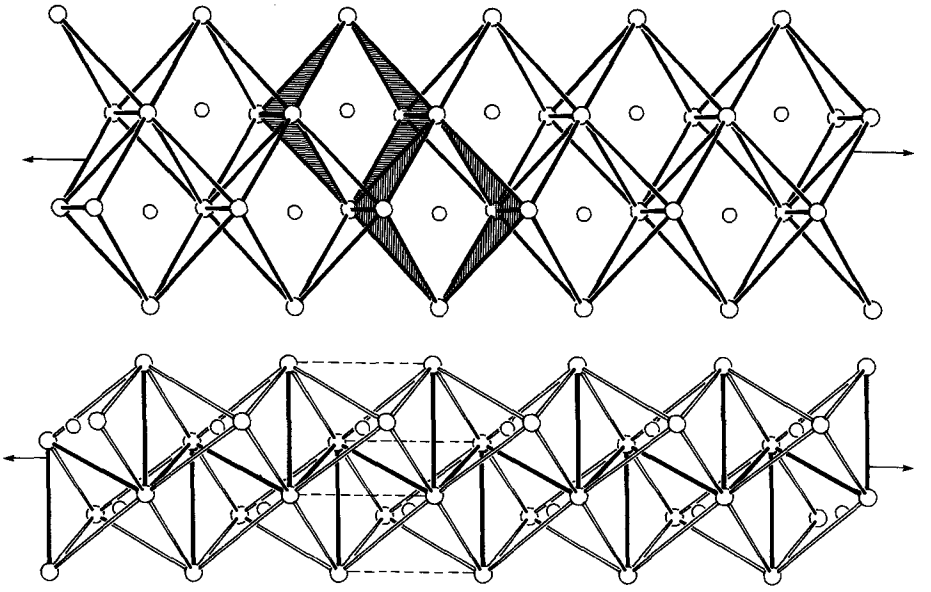

FIG. 2. Two approximately normal views of the chain of metal octahedra in $Sc_7Cl_{10}C_2$ together with the centered carbon atoms. The 8% longer repeat along the chain repeat (3.50 Å) is omitted for clarity. Shared edges between octahedra are in heavy outline in the lower view.

ces of the chlorine octahedra also bridge the side edges of the metal chain (Sc3–Sc3′), while the shared Cl5 atoms are exo to each vertex of the metal chain at Sc2. Partition of the latter according to metal neighbors gives an approximate description as $^1_\infty[(Sc^{III}Cl_2)(Sc_6Cl_8)]$.

Bonding and nearest neighbor nonbonding distances are given in Table IV together with the corresponding distances in Sc_7Cl_{10}. The metal chains in the two structures are closely comparable, the presence of scandium–carbon bonding generally giving smaller and somewhat more regular metal polyhedra. Neglecting the long repeat distances for all atoms along the chain at ca. 3.50 Å, the average Sc–Sc distance here is 3.24 Å, 0.03 Å less than without carbon, with the shared edges still the shortest, as is typical. The Sc3–Sc4 joins within the octahedral chains now alternate with carbon atoms and at 3.07 Å are 0.05 Å shorter than in Sc_7Cl_{10}. A more striking effect is a 0.105-Å decrease in Sc3–Sc4[b]. (The actual distances within the octahedra, neglecting the long repeat, still vary over a range of 0.23 Å or by 14%.)

The scandium–chlorine distances show nothing unusual although slightly shorter values for bridging chlorine on the chain are to those scandium atoms that are more exposed and have fewer metal neighbors. On the other hand, Cl–Cl repulsions may be responsible; clusters and extended arrays are characteristically well-sheathed by the nonmetal (*26*), and the longer Sc–Cl distances for Cl1,2,4 correlate quite well with the probable distortions arising from the shorter Cl–Cl separations (Table IV). The exo Sc–Cl distances are characteristically longer and also appear to be limited by Cl–Cl contacts.

The Sc–C distances seem quite reasonable, the 2.31-Å average here comparing very well with 2.308(1) Å (×6) in Sc_2Cl_2C (*10, 11*). The so-called monocarbide (NaCl type) is carbon-deficient with a composition near Sc_2C and a lattice constant for an ap-

TABLE IV
DISTANCES (Å) IN $Sc_7Cl_{10}C_2$ AND IN Sc_7Cl_{10}[a]

	$Sc_7Cl_{10}C_2$	Sc_7Cl_{10}
Scandium in chain		
Sc2–Sc3	3.245 (1)	3.253 (2)
Sc2–Sc4	3.290 (1)	3.271 (2)
Sc3–Sc4	3.072 (2)	3.147 (3)
Sc3–Sc4[b]	3.302 (1)	3.407 (3)
Sc4–Sc4[b]	3.131 (2)	3.153 (3)
Sc1–Sc1[c]	3.4930 (4)	3.5366 (6)
Chlorine on metal chain		
Sc4–Cl1	2.658 (2)	2.695 (2)
Sc2–Cl1	2.510 (1)	2.443 (3)
Sc4[b]–Cl2	2.625 (1)	2.627 (3)
Sc3–Cl2	2.499 (2)	2.570 (2)
Sc2–Cl4	2.539 (1)	2.487 (3)
Sc3–Cl4	2.601 (2)	2.631 (2)
Bridging chlorine		
Sc3–Cl3	2.666 (1)	3.208 (4)
Sc1–Cl3	2.560 (2)	2.502 (2)
Sc2–Cl5	2.799 (2)	2.611 (3)
Sc1[d]–Cl5	2.539 (1)	2.566 (3)
Carbon in chain		
Sc2–C	2.185 (6)	
Sc3–C (×2)	2.284 (4)	
Sc4–C (×2)	2.375 (4)	
Sc4–C	2.339 (6)	
Chlorine–chlorine[c,e]		
Cl1–Cl2[b]	3.443 (6)	3.460
Cl1–Cl5	3.516 (6)	3.910
Cl3–Cl4	3.520 (6)	3.443
Cl4–Cl5	3.530 (6)	3.698
Cl2–Cl3	3.557 (6)	3.452
Cl1–Cl2[f]	3.560 (6)	3.910

[a] Ref. (*16*).
[b] $1/2 - x$, $1/2 - y$, $1 - z$.
[c] All atoms repeat at the b axis length.
[d] $1/2 - x$, $1/2 - y$, z.
[e] ≤3.560 Å.
[f] Interchain distance.

parent NaCl-type subcell that corresponds to 2.36 Å for Sc–C; the well-described Sc_4C_3 (anti-Th_3P_4 type) has an average Sc–C distance of 2.24 Å (*27*).

Structure Comparisons

Sc_7Cl_{10}. As described above, the double-metal chains in the phase $Sc_7Cl_{10}C_2$ shows a remarkable similarity to those in Sc_7Cl_{10}. The remainder of the structure is distinctly different, however. Figure 3 compares Sc_7Cl_{10} (left) and $Sc_7Cl_{10}C_2$ (right) in projection along the short b axes, with dotted atoms differing from open circles by $b/2$. The chlorine elevations in the two views are taken to be the same. Their disposition about the scandium chain is such as to cap exposed triangular *faces* in Sc_7Cl_{10} but to bridge *edges* in $Sc_7Cl_{10}C_2$, the change also being accompanied by the rotation of the isolated scandium(III) chains by ~70°. The conversion of Sc_7Cl_{10} to $Sc_7Cl_{10}C_2$ (or vice versa) can thus be accomplished by displacement of all metal atoms in the structure by $b/2$ together with changes in the x and z coordinates of Cl3 and Cl5 so as to reestablish reasonable distances within shared chloride octahedra, the displacement of Sc1 serving to interconvert waist and apex functions. The clear change in chlorine placement about the exposed metal vertices of the chain on conversion from face to edge bridging chlorine (Fig. 3) lengthens the Sc2–Cl5 interchain link by 0.19 Å, but causes a more drastic shortening of the Sc3–Cl3 bridging by 0.54 Å owing to a clearly greater obstruction of the Sc3 vertex in the metal chain by chlorine atoms in Sc_7Cl_{10}. Much of the 6.8% decrease in cell volume accompanying the carbon addition can be associated with a decrease in height of the metal chain from carbon bonding together with tighter Sc3–Cl3 bridging and thence smaller separations between metal chains.

A fairly simple explanation can be discerned for the change from face- to edge-bridging chlorine around the metal chains on introduction of carbon into the cluster, the reduction of carbon–chlorine interactions. The cluster centers in Sc_7Cl_{10} are only 2.88 and 3.01 Å from Cl2 and Cl4, respectively, or 2.86 and 2.89 Å in a model with a carbide-like metal chain in the Sc_7Cl_{10} arrangement, while the observed C–

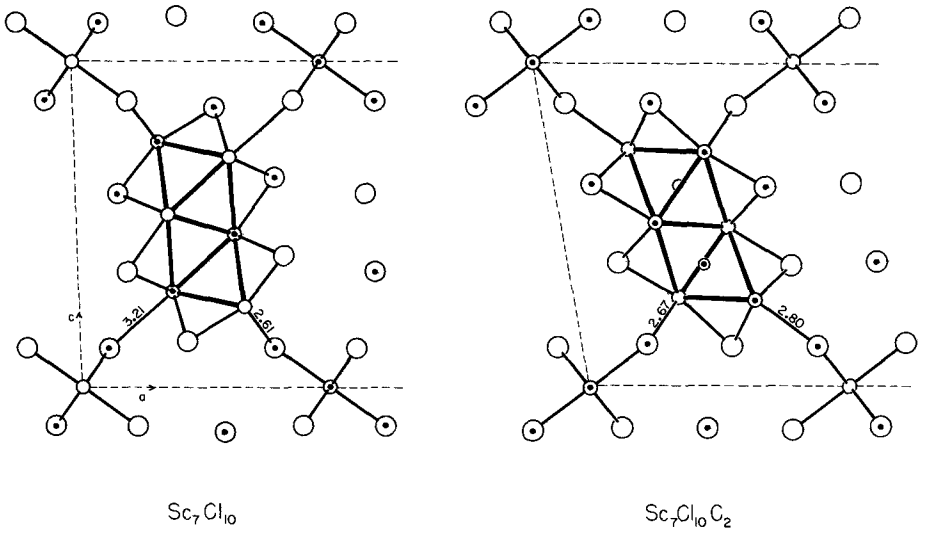

FIG. 3. Comparison of the Sc_7Cl_{10} (left) (*17*) and $Sc_7Cl_{10}C_2$ (right) structures in projection along the metal chain with dotted atoms separated by *b*/2 from the remainder. The two structures may be interconverted by displacement of all metal atoms by *b*/2, changing the chlorine on the metal chain from face-capping to edge-bridging functions.

Cl separation in $Sc_7Cl_{10}C_2$ is 3.48 Å, the same as in Sc_2Cl_2C. The former separations seem to be well less than the sum of reasonable van der Waals radii when it is noted that chlorine is the order of 1.75 Å in radius to other chlorines (Table IV). An electrostatic argument can also be used since both chlorine and carbon presumably bear some negative charge. Calculation of the Madelung part of the lattice energy (MAPLE) (*28*) for several different charge distributions indicate that the observed structure has up to a few percent greater lattice energy as well as a more uniform contribution to that by the three types of scandium atoms in the chain. In general, structures with metal octahedra that are face-capped by nonmetal are more likely to be destabilized by repulsions between the nonmetal and interstitial atoms centered in metal octahedra. The structures of Gd_2Cl_3, Nb_6I_{11}, and Zr*X* are also of this type, while a much larger number of clusters and chains contain face-capping halide. The transition from 3R-Zr*X* structures to the 1T-type as in Sc_2Cl_2C on insertion of nonmetal into the octahedral site (below) is exactly analogous to the transition discussed here in terms of diminished halogen–interstitial interactions.

The new carbide phase also bears a considerable similarity to Sc_7Cl_{10} in that it too exhibits significant variations in cell dimensions. About 16 sets of lattice constants have been refined for different preparations of $Sc_7Cl_{10}C_2$ using 16 to 27 Guinier reflections from each measured relative to powdered silicon as an internal standard. Seventy percent of these gave cell volumes within ± 1.1 Å^3 of the 757.5-Å^3 average for the second and third crystals studied by single-crystal means, the extremes in fact occurring for products of high-yield reactions. The remaining cell volumes grouped in the range of 761.3 to 763.4 Å^3 with the first crystal used to determine the structure providing the upper limit. Since members of this last group generally were found early in the investigation, some consideration was given to the presence of a different intersti-

TABLE V

SCANDIUM COORDINATION NUMBERS AND SCANDIUM–CARBON DISTANCES IN $Sc_7Cl_{10}C_2$

Scandium atom	Coordination number[a,b]			Distance Sc–C (Å)
	To Sc	To Cl	To C	
1	0	6	0	
2	4	5	1	2.18
3	5	4	2	2.28 (×2)
4	7	3	3	2.34
				2.38 (×2)

[a] To all first neighbors listed in Table IV; all atoms have two additional neighbors of like kind at 3.49 Å, the *b* axis repeat.

[b] Sc_7Cl_{10} has the same coordination for Sc and Cl except for four Cl about Sc2; Sc_5Cl_8 is the same lacking Sc4.

tial atom or a mixture, although subsequent attempts to insert boron, nitrogen, or oxygen alone in this structure have been unsuccessful. However, a close comparison of the actual structural data from crystal one with that of crystal two (the better) suggests changes in crystal perfection may be responsible instead, the first being the poorer judging from Weissenberg films. In addition, the apparent thermal ellipsoids obtained for metal in the first crystal refinement were uniformly about twice as large and with standard deviations 15–20% greater than for the second. Likewise, thermal parameters for chlorine were about 10% larger and B_{22} for the isolated Sc1 was 50% greater. In addition, the Sc–Sc distances within the chain were all 0.02 to 0.03 Å larger, but with Sc–Cl differences larger by no more than 0.01 Å and generally not significantly so. These observations are remarkably similar to those made earlier with respect to two different crystals of Sc_7Cl_{10} (*17*) even as to the relative sizes of the ellipsoids for Cl3 and Cl5. Since there was no evidence whatsoever for interstitial atoms in the earlier structural results for Sc_7Cl_{10}, we are inclined to prefer the same explanation for the present variations, that is, intrinsic differences in imperfections among crystals with very anisotropic bonding. Whether hydrogen might cause such changes is still under investigation.

Several aspects of the carbon bonding bear comment. At first glance the Sc–C distances (Table IV) seem quite irregular, but these turn out to vary plausibly with the total amount of bonding that can be inferred for each scandium atom based on distances. The metal octahedra are elongated along *b* and compressed normal to this along the shared edge Sc3–Sc4. The carbon is actually displaced ~0.12 Å in *c* from the waist of the octahedron toward Sc2 and Sc3 to produce the order $2 < 3 < 4^b < 4$ in distances to scandium. As seen in the coordination number summary in Table V, this follows precisely the change in environment of scandium, there being closer carbon contacts with those metal atoms that have more chlorine and fewer scandium neighbors and therefore perhaps a higher charge. The introduction of carbon is also seen to produce a remarkable uniformity, six nonmetal nearest neighbors for all scandium atoms.

The process of cluster formation and condensation generally involves replacement of part of the chlorine about each metal in the parent halide, six in the case of the $ScCl_3$, by a greater number of metal atoms, i.e., five Sc substitute for two Cl on average to form the present structure, nine Sc for three Cl for ScCl (*19*), and finally twelve for all six in the metal. The Sc–Cl separations remain remarkably constant throughout this, the additional electrons generally not screening the Sc–Cl separations significantly, while the added and more numerous metals that replace chlorine occur at relatively long Sc–Sc distances compared with the single-bond metal radius (2.92 Å). The metal-bonded halides indeed appear to possess just exactly the distance-coordination number intermedi-

acy that one would expect between a salt and a delocalized metal (*29*).

Er_7I_{10}. Although the isomorphous relationship between $Sc_7Cl_{10}C_2$ and Er_7I_{10} does not immediately require that an interstitial impurity exists in the latter, some factors suggest this may be true. The iodide (*24*) was obtained in only small and irregular yields and showed some similar crystallographic problems, namely, a very elongated ellipsoid along *b* (>3 : 1) for an isolated ErI atom with a refined occupancy of only 0.70. There was also a prominent residual in the middle of all metal octahedra that refined to 0.25 of an iodine ($R = 0.055$). The authors noted that this site was also the position of a missing halogen atom in otherwise approximately close-packed layers that run parallel to (100) and that disorder or phasing errors might therefore contribute a false peak at this point. Extinction was said to be clearly evident but not corrected for, a condition that we have found can also lead to appreciable errors in Fourier synthesis maps.

Efficient filling of space allows a good number of these structures to be described in terms of close-packed anion arrays in which clustering of metal atoms in adjoining octahedral interstices occurs around a missing anion at the cluster center (*17, 24, 30*). This can be seen well in Fig. 2 in planes that run parallel to (001) for Sc_7Cl_{10} and $Sc_7Cl_{10}C_2$, closer to the ideal in the latter. Interestingly, the best close-packed planes in Er_7I_{10} lie parallel to (100) instead (*24*) even though the last two compounds are nominally isomorphous in terms of relative atom positions and metal-halide placement. The metal chains in the two are quite similar, but the difference in the size of both atoms causes appreciable changes in the relative orientation of the metal and halogen chains, the interconnections between them showing some flexibility. Thus, the interchain placement defined by the angle between Sc1–Cl3 and Sc3–Sc2^b differs by somewhat over 30° between the two. Under the circumstances a close-packed description does not seem particularly useful.

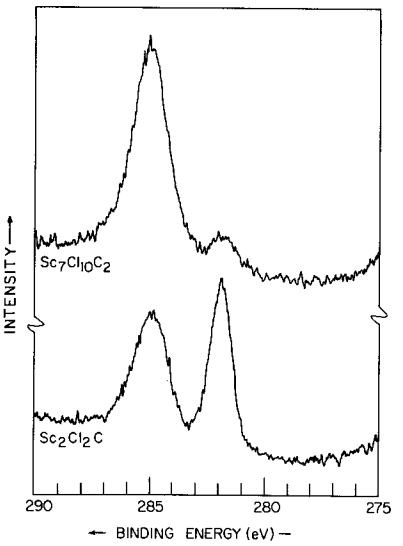

FIG. 4. The carbon 1*s* photoelectron spectra of $Sc_7Cl_{10}C_2$ and Sc_2Cl_2C (*11*) on cellophane tape (Al$K\alpha$).

Photoelectron Spectroscopy

Since X-ray scattering is relatively unspecific as to identity of the interstitial atom, it was considered desirable to establish that interstitial-like carbon was actually present in the new phase. Figure 4 shows the carbon 1*s* spectrum (Al$K\alpha$) from $Sc_7Cl_{10}C_2$ relative to that of Sc_2Cl_2C where carbon is bound in octahedral interstices between double-metal-layers (*10, 11*). Clearly both samples are very similar in this respect with a carbide-like peak shifted about 3.1 eV to lower binding energy from the inevitable adventitious carbon used for calibration (≡285.0 eV). (The powdered $Sc_7Cl_{10}C_2$ had been handled first in a prep box where it had been exposed to more abundant hydrocarbon impurities. Experience (*31*) indicates that this source dominates emission from the cellophane-tape substrate when good coverage is secured al-

TABLE VI

X-RAY PHOTOELECTRON EMISSION DATA, eV[a]

	Sc	Sc_7Cl_{10}	$Sc_7Cl_{10}C_2$	Sc_2Cl_2C[b]	$ScCl_3$[c]
Cl $3p$		7.0	6.6		6.4
Sc*m*[d] $2p_{3/2}$	398.7	398.8	401.0	400.8	
$2p_{1/2}$	403.4	~403.4	~405.5	405.6	
Sc*n* $2p_{3/2}$		~403.9	~403.3		404.0
$2p_{1/2}$		408.3	~407.7		408.5
Cl $2p_{3/2}$		200.2	199.9	200.0	200.1
Sc*m* $2p_{3/2}$–Cl $2p_{3/2}$		198.6	201.1	200.8	
Sc*n* $2p_{3/2}$–Cl $2p_{3/2}$		203.7	203.4		203.9

[a] Referenced to C(1*s*) = 285.0 eV.

[b] Ref. (*11*).

[c] Calibrated with deposited gold, $4f_{7/2}$ = 84.0 eV.

[d] The pair of Sc $2p$ transitions *m* in Sc_7Cl_{10} and $Sc_7Cl_{10}C_2$ with the lower binding energy is assigned to metal chain, while the *n* pair is taken to originate with the isolated scandium(III).

though the two sources generally cannot be distinguished unless sample charging occurs.)

Other pertinent XPS data for Sc_7Cl_{10}, $Sc_7Cl_{10}C_2$, Sc_2Cl_2C, $ScCl_3$, and Sc are summarized in Table VI. The scandium $2p$ core peaks for Sc_7Cl_{10} and $Sc_7Cl_{10}C_2$ present an interesting relationship. As shown in Fig. 5, the older Sc $2p$ spectrum for Sc_7Cl_{10} (top)

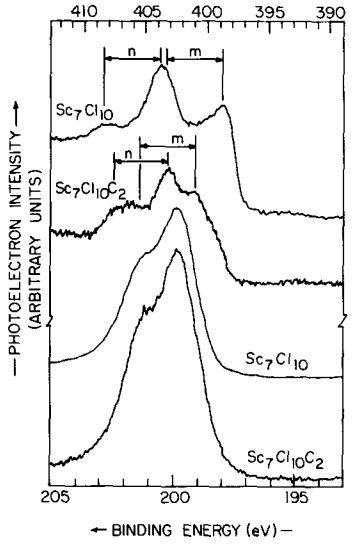

FIG. 5. Scandium and chlorine $2p$ spectra in Sc_7Cl_{10} and $Sc_7Cl_{10}C_2$ with Sc $2p_{3/2-1/2}$ assignments for the metal chain (*m*) and scandium(III) (*n*) states.

has been given a somewhat tentative assignment in terms of the two kinds of scandium known to occur in the compound, a broadened $2p_{3/2}$–$2p_{1/2}$ pair (*m*) starting at about 399 eV for the collection of metal in the metal chains together with a smaller overlapping pair (*n*) from the isolated chain at ~404 eV (*32*). Although possible alternatives in terms of shake-up (secondary) processes made the earlier assignment seem a little tenuous, quite similar results are obtained for $Sc_7Cl_{10}C_2$ and this encourages the spectral comparison and assignments shown. Some surface oxidation may also contribute to *n*.

The 3/2–1/2 pairs of Sc $2p$ transitions so assigned to the metal and scandium(III) chains in Sc_7Cl_{10} are found to agree very well with the energies of these emissions obtained for the metal and the trichloride, respectively. The metal chain in $Sc_7Cl_{10}C_2$ is clearly more oxidized as these Sc $2p$ binding energies increase ~2 eV while the other pair assigned to the isolated atom change only ~0.6 eV, in the opposite direction in fact. The metal $2p$ energies in $Sc_7Cl_{10}C_2$ are also very comparable to those found for Sc_2Cl_2C, which is formally a scandium(III) compound. Of course, general comparisons of this sort may be misleading in that the apparent changes in core levels to higher binding energy on oxidation may actually reflect more of the natural shift of the Fermi level reference to higher values (*31*). This can be avoided by comparing changes in the scandium $2p_{3/2}$ energies with those for chlorine $2p_{3/2}$ as an internal standard, which for the present examples leaves the conclusions relatively unaffected (Table VI).

Finally, Fig. 6 compares the XPS results for the valence region of Sc_7Cl_{10} and $Sc_7Cl_{10}C_2$. A metal band in the neighborhood of 0–3 eV with an edge at or near E_F is indicated for Sc_7Cl_{10}, a feature that is more distinct at 0–3.5 eV in the He(I) spectrum (*32*). On the other hand, a metal band is

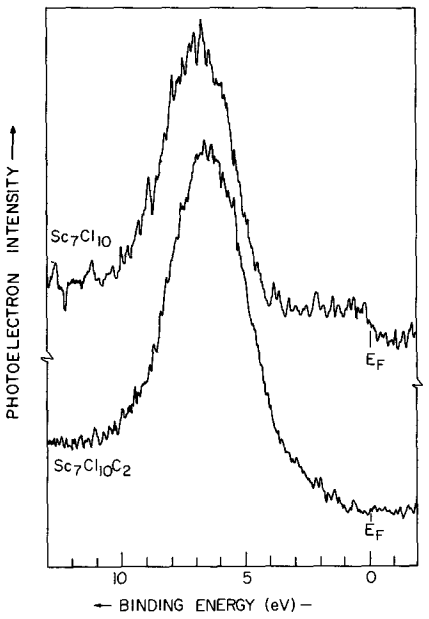

FIG. 6. Valence spectra of Sc_7Cl_{10} and $Sc_7Cl_{10}C_2$ (Al$K\alpha$).

either absent or greatly reduced in $Sc_7Cl_{10}C_2$ according to the XPS results. One can imagine instead some broadening in the neighborhood of 3 eV corresponding to the nominal C 2*p* band, particularly with the knowledge that such a feature clearly appears at 3.6 and 4.3 eV in Sc_2Cl_2C and Zr_2Cl_2C, respectively (*3, 11*), where the carbon content is higher.

Interstitial Atoms

Although a good number of clusters and infinite metal-bonded arrays formed by metals of transition groups III and IV appear quite free of interstitial atoms from the second or higher periods—Sc_5Cl_8, Sc_7Cl_{10}, ScCl, Y_2Cl_3, YCl, and ZrCl, for example (*26, 29*)—a number of others in addition to $Sc_7Cl_{10}C_2$ appear to be stabilized by a small second-period nonmetal. The previously reported $Sc(Sc_6Cl_{12})$ (*33*) is of this character as it exhibited the characteristic problems of an unreproducible synthesis with low yields at best and a structure solution with a small electron density residual at the cluster center ($Z \sim 5.3$). General recognition of the likelihood that adventitious impurities rather than errors in the crystallographic data or their analysis may be responsible in such instances has led us to the purposeful additions of a variety of potential impurities to synthetic experiments. In the case of Sc_7Cl_{12}, nitrogen was discovered to give the same phase, $Sc(Sc_6Cl_{12}N)$, in good yield (*3*).

The possibility of interstitial bonding of nonmetals between the double-metal-layers in the zirconium monohalide structures has also been explored without the impetus of a serendipitous discovery. This led first to the insertion of hydrogen and oxygen in the tetrahedral metal sites in the zirconium phases (*8, 12*) and subsequently to success with hydrogen, nitrogen, carbon, and boron (Z), these going primarily into octahedral sites to form phases of composition M_2X_2Z (M = Zr, Sc, Y) or ZrXH in either one- (1T) or three-slab (3R) structures. Some results are summarized in Table VII to illustrate the breadth of the chemistry. All of these involve two-phase reactions except with oxygen and possibly nitrogen in tetrahedral

TABLE VII

INTERSTITIAL DERIVATIVES OF DOUBLE-METAL-LAYERED MX PHASES

	Formal M–M bonding e's/M[a]	Ref.
Tetrahedral sites		
H: 3R–ScClH, YClH	1	*3, 9*
M–ZrXH$_{0.5}$[b]	2.5	*8*
O: 3R–$ZrClO_{0.43}$, $ZrBrO_{0.35}$	~2.2	*12*
N: 3R–$ZrClN_{1-x}$	3×	*34*
Octahedral sites		
H: 1T–ZrXH (X = Cl, Br)	2	*9*
N: 1T–Zr_2Cl_2N	1.5	*34*
1T–Sc_2Cl_2N	0.5	*3*
C: 1T–Zr_2X_2C	1	*11*
1T–, 3R–Sc_2Cl_2C, 1T–Y_2Cl_2C	0	*3, 10*
B: 1T–Zr_2Cl_2B	0.5	*34*

[a] The electron count after filling the anion band.
[b] Monoclinic.

interstices in Zr*X* where the uptake occurs within a single phase, quite analogous to their behavior in zirconium metal itself (*12*). The occurrence of carbon atoms in condensed gadolinium halide clusters has also been noted (*4*).

The bonding of the nonmetal in these appears to be strong and the stabilizing effect appreciable since Sc_7Cl_{12}, edge-bridged Sc_7Cl_{10}, and 1T-*MX* phases, for example, are not found otherwise. The separation of the double-metal-layers in ScCl is significantly decreased on formation of Sc_2Cl_2C. Some feeling for the bonding in $Sc_7Cl_{10}C_2$ can be obtained from the results of extended Hückel calculations on some of the centered clusters and on Zr_2Cl_2C. The metal-based molecular orbitals for an isolated (or shared) M_6 cluster will always include bonding combinations of metal orbitals that transform the same as the 2*s* and 2*p* orbitals on a centered, interstitial atom. For the elements considered, these will combine to produce four bonding levels that lie significantly below both the metal cluster M.O.'s and the interstitial atom A.O.'s. Full occupation of the new and more bonding levels means that a carbon interstitial and the metal-based system each provide four orbitals and four electrons to fill the new band, four new and high-lying antibonding orbitals also appearing. The occupied, bonding levels derived from carbon 2*p* (plus Zr, of course) lie 4.3 eV below E_F in Zr_2Cl_2C vs 2.0 eV for the metal *d* band maximum in ZrCl (*11, 15*). These bonding orbitals involve substantial mixing of metal and carbon and are bonding for both metal–metal and metal–carbon, more so for the latter. It is misleading to think of the interstitial as C^{4-} in character although the familiar process of electron counting for oxidation state assignment or filling of valence bands may be so misconstrued. Extensive band calculations on the rock-salt monocarbides of Ti, Zr, V, and Nb emphasize both the metal–carbon covalency and the small negative charge acquired by carbon, estimated values for the latter lying between 0.4 and 1 (*35, 36*). The 3.0-eV difference in Sc 2*p* binding energy found between Sc_2Cl_2C and $ScCl_3$ for either a Cl 2*p* or E_F reference (Table VI) is striking evidence for the Sc–C covalency. In fact, the compound $Sc_7Cl_{10}C_2$ with an average oxidation state of 2.57 is indistinguishable from Sc_2Cl_2C by this means. The covalency and electron redistribution on formation of metal hydrides such as Zr*X*H and ZrH_2 are conceptually quite similar, the comparable XPS shift being ~1 eV (*15*). Qualitative features of the bonding scheme have been described by Lauher for metal carbonyl carbide clusters (*37*).

In the case of Zr_2Cl_2C there is still one electron per metal atom left in the metal conduction band after the valence bands are filled, and the phase is metallic both by XPS and by theory (*10*), while $Sc_7Cl_{10}C_2$ and Sc_2Cl_2C (a valence compound) both appear to be semiconductors by XPS, the highest levels in the latter probably being carbon 2*p* (plus Sc) in character and well separated from E_F. This last condition is not always the case, ZrC, for example, being metallic through overlap of the valence and conduction bands (for more discussion see (*16, 35*)). Studies of the more favorable ultraviolet photoelectron spectrum of $Sc_7Cl_{10}C_2$ are planned in an attempt to clarify the locations of the carbon-generated and metal valence bands.

Acknowledgments

The authors are indebted to J. W. Anderegg for measurement of the photoelectron emission spectra of the reduced systems, to R. J. Thorn (Argonne) for XPS data for Sc and $ScCl_3$, to R. A. Jacobson for the availability of excellent X-Ray diffraction and computational facilities, and to G. Meyer for the MAPLE calculations on different models of $Sc_7Cl_{10}C_2$.

References

1. A. Simon, *Z. Anorg. Allg. Chem.* **355**, 311 (1967).

2. H. IMOTO AND J. D. CORBETT, *Inorg. Chem.* **19,** 1241 (1980).
3. S.-J. HWU AND J. D. CORBETT, unpublished research (1984).
4. E. WARKENTIN AND A. SIMON, *Rev. Chem. Miner.* **21,** 488 (1984).
5. E. WARKENTIN AND A. SIMON, unpublished research (1983).
6. E. WARKENTIN, R. MASSE, AND A. SIMON, *Z. Anorg. Allg. Chem.* **491,** 323 (1982).
7. A. SIMON AND E. WARKENTIN, *Z. Anorg. Allg. Chem.* **497,** 79 (1983).
8. H. S. MAREK, J. D. CORBETT, AND R. L. DAAKE, *J. Less-Common Met.* **89,** 243 (1983).
9. S. WIJEYESEKERA AND J. D. CORBETT, unpublished research.
10. J. E. FORD, J. D. CORBETT, AND S.-J. HWU, *Inorg. Chem.* **22,** 2789 (1983).
11. R. P. ZIEBARTH, S. V. WINBUSH, S.-J. HWU, J. E. FORD, AND J. D. CORBETT, submitted for publication.
12. L. M. SEAVERSON AND J. D. CORBETT, *Inorg. Chem.* **22,** 3202 (1983).
13. A. SIMON, private communication, 1983.
14. E. FROMM AND E. GEBHARDT, "Gase und Kohlenstoff in Metallen," Springer-Verlag, Heidelberg, West Germany (1976).
15. J. D. CORBETT AND H. S. MAREK, *Inorg. Chem.* **22,** 3194 (1983).
16. S. WIJEYESEKERA AND R. HOFFMANN, *Organometallics* **3,** 949 (1984).
17. K. R. POEPPELMEIER AND J. D. CORBETT, *Inorg. Chem.* **16,** 1107 (1977).
18. K. R. POEPPELMEIER AND J. D. CORBETT, *J. Amer. Chem. Soc.* **100,** 5039 (1978).
19. K. R. POEPPELMEIER AND J. D. CORBETT, *Inorg. Chem.* **16,** 294 (1977).
20. J. D. CORBETT, *Inorg. Synth.* **22,** 15, 39 (1983).
21. R. L. LAPP AND R. A. JACOBSON, DOE Report IS-4708, Ames Laboratory, Iowa State University (1979).
22. D. R. POWELL AND R. A. JACOBSON, DOE Report IS-4737, Ames Laboratory, Iowa State University (1980).
23. D. S. RUSTAD AND N. W. GREGORY, *Inorg. Chem.* **21,** 2929 (1982).
24. K. BERROTH AND A. SIMON, *J. Less-Common Met.* **76,** 41 (1981).
25. B. A. KARCHER, Ph.D. dissertation, Iowa State University (1981).
26. J. D. CORBETT, *Adv. Chem. Ser.* **186,** 329 (1980).
27. N. H. KRIKORIAN, A. L. BOWMAN, AND M. C. KRUPKA, *High-Temp. Sci.* **1,** 360 (1969).
28. R. HOPPE, *Angew. Chem.* **20,** 70 (1981).
29. J. D. CORBETT, *Pure Appl. Chem.* **56,** 1527 (1984).
30. A. SIMON, *Angew. Chem. Int. Ed. Engl.* **20,** 1 (1981).
31. J. D. CORBETT, G. MEYER AND J. W. ANDEREGG, *Inorg. Chem.* **23,** 2625 (1984).
32. K. R. POEPPELMEIER, Ph.D. thesis, Iowa State University (1977).
33. J. D. CORBETT, K. R. POEPPELMEIER, AND R. L. DAAKE, *Z. Anorg. Allg. Chem.* **491,** 51 (1982).
34. R. P. ZIEBARTH AND J. D. CORBETT, unpublished research.
35. A. NECKEL, *Int. J. Quant. Chem.* **23,** 1317 (1983).
36. B. M. KLEIN, D. A. PAPACONSTANTOPOULOS, AND L. L. BOYER, *Phys. Rev. B* **22,** 1946 (1980).
37. J. W. LAUHER, *J. Amer. Chem. Soc.* **100,** 5305 (1978).